

## ARTICLE

DOI: 10.1038/s42004-018-0067-2

OPEN

# Imidazolate ionic liquids for high-capacity capture and reliable storage of iodine

Ruipeng Li<sup>1</sup>, Yanfei Zhao<sup>2</sup>, Yu Chen<sup>2</sup>, Zhimin Liu<sup>2</sup>, Buxing Han<sup>2</sup>, Zhiyong Li<sup>1</sup> & Jianji Wang<sup>1</sup>

Fast, efficient capture and safe storage of radioactive iodine is of great significance in nuclear energy utilization but still remains a challenge. Here we report imidazolate ionic liquids (Im-ILs) for rapid and efficient capture, and reliable storage of iodine. These Im-ILs can chemically capture iodine to form I-substituted imidazolate ILs with an iodide counterion and the newly formed ILs can absorb iodine to form polyiodide species and low-temperature eutectic salts. For example, choline imidazolate shows iodine capture capacities of 8.7 and 17.5 g of iodine per gram of IL at 30 and 100 °C, respectively, which are, to the best of our knowledge, higher than the values (0.5–4.3 g/g) reported to date. Importantly, iodine can be stably stored in the Im-IL absorbent systems even at 100 °C. The Im-ILs have potential for application in the capture and storage of radioactive iodine.

<sup>1</sup>Key Laboratory of Green Chemical Media and Reactions, Ministry of Education, School of Chemistry and Chemical Engineering, Henan Normal University, Xinxiang, Henan 453007, China. <sup>2</sup>CAS Key Laboratory of Colloid, Interface and Thermodynamics, Beijing National Laboratory for Molecular Sciences, Institute of Chemistry, Chinese Academy of Sciences, Beijing 100190, China. These authors contributed equally: Ruipeng Li, Yanfei Zhao. Correspondence and requests for materials should be addressed to Z.L. (email: [liuzm@iccas.ac.cn](mailto:liuzm@iccas.ac.cn)) or to J.W. (email: [jwang@htu.cn](mailto:jwang@htu.cn))

Nuclear energy, a clean and low carbon-emitting power resource, is an efficient and reliable alternative source to fossil energy if the challenge of nuclear waste pollution can be tackled efficaciously<sup>1,2</sup>. Appropriate nuclear waste management has received considerable attention especially after the explosion of the Fukushima nuclear power plant in 2011. Volatile and radioactive iodine species (e.g., <sup>129</sup>I and <sup>131</sup>I) possess exceptional issues, mainly because <sup>129</sup>I has a very long half-life (~10<sup>7</sup> years) and <sup>131</sup>I has direct effects on human metabolic processes despite its short half-life (8.02 days). Therefore, efficient capture and reliable storage of radioactive I<sub>2</sub> is of great significance. To realize the effective I<sub>2</sub> capture, great efforts have been devoted to developing various physico- and chemo- adsorbents/adsorbents. Metal-organic frameworks<sup>3-5</sup>, microporous polymer<sup>6-8</sup>, charged porous aromatic frameworks<sup>9</sup>, hydrogen-bonded cross-linked organic framework<sup>10</sup>, nonporous pillar[6] arene crystal<sup>11</sup>, carbon-based materials<sup>12,13</sup>, deep eutectic solvents<sup>14</sup>, and ionic liquids (ILs)<sup>15-17</sup>, have been reported for the efficient capture of I<sub>2</sub> via physical interaction. However, these materials usually suffer from low I<sub>2</sub> uptake and unstable I<sub>2</sub> storage. Ag<sub>2</sub>O@NFC aerogels<sup>18</sup>, silver-containing mordenites<sup>19</sup>, alkene/alkyne perovskites<sup>20</sup>, alkali-TCNQ salts<sup>21</sup>, and functionalized Mg-Al layered double hydroxide<sup>22</sup> have been reported as chemical adsorbents, whose capture efficiency are considerably dependent on their activity to react with I<sub>2</sub>, generally with shortcomings such as slow reaction rate and low capture capacity. Consequently, although such progress has been made in I<sub>2</sub> capture, the adsorbents/adsorbents capable of fast capturing and reliably storing I<sub>2</sub> is still highly desirable.

ILs, composed entirely of organic cations and inorganic/organic anions, can be designed with specific and tunable chemical reactivity via careful selection of component ions, and have been widely applied in gas capture and chemical wastes management, showing promising potentials<sup>23-25</sup>. For example, 1-butyl-3-methylimidazolium tetrafluoroborate/water system has

been demonstrated to be a tunable media for sustainable waste management<sup>26</sup>. Heterocyclic anions-based ILs, including azolate and pyridinolate ILs, have been reported as efficient sorbents for CO<sub>2</sub>, SO<sub>2</sub>, or NO due to the formation of complexes between the ILs and the gases<sup>27-32</sup>. Especially, the azolate and pyridinolate anions of the ILs have been found to be capable of chemically capturing CO<sub>2</sub> efficiently<sup>27-29</sup>. ILs also have been applied in I<sub>2</sub> capture and 1-butyl-3-methylimidazolium bromide was reported to show an I<sub>2</sub> capture capacity of 1.9 mol I<sub>2</sub> per molar IL<sup>15</sup>.

Here we report a series of imidazolate ILs (Im-ILs) for fast capture and reliable storage of I<sub>2</sub>. These Im-ILs are capable of chemically capturing I<sub>2</sub> rapidly via the reaction of the Im anions with I<sub>2</sub>, forming I-substituted imidazoles together with new ILs with [I]<sup>-</sup> anion, and the in situ-generated ILs can absorb I<sub>2</sub> to form polyiodide species, resulting in very high I<sub>2</sub> uptake capacity. For example, choline imidazolate ([Ch][Im]) as the initial adsorbent shows increased I<sub>2</sub> capture capacities with temperature in the range of 30–100 °C, giving the capacities of 8.7 and 17.5 g of I<sub>2</sub> per gram IL at 30 and 100 °C, respectively, which is an improvement over typical state-of-the-art capacities of 0.5–4.3 g/g. More importantly, the captured I<sub>2</sub> can be stably stored in the adsorbent system even at 100 °C. It is suggested that the Im-ILs reported here are highly efficient not only for fast capture of I<sub>2</sub> with high capacity, but also for the safe storage of this volatile compound.

## Results

**Synthesis and characterization of Im-ILs.** The Im-ILs shown in Fig. 1a were synthesized via the neutralization of bases (e.g. choline) with weak proton donors including imidazole (Im), methyl-substituted Im, as detailed in the Methods. The <sup>1</sup>H and <sup>13</sup>C nuclear magnetic resonance (NMR) spectra confirmed the formation of these Im-ILs (Supplementary Fig. 1), and thermogravimetric analysis (TGA) showed that they are thermally stable from 131 °C to 223 °C (Supplementary Fig. 2). These Im-ILs are

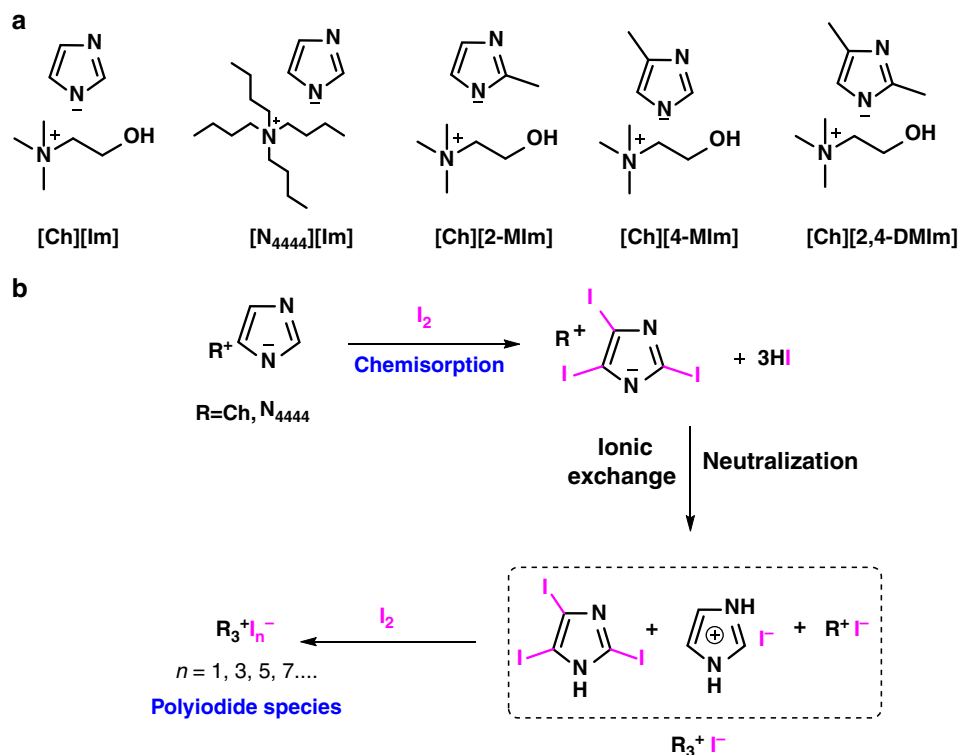


**Fig. 1** Structure and function of Im-ILs. Chemical structures of Im-ILs (**a**) and possible pathway of I<sub>2</sub> capture by R<sup>+</sup>[Im]<sup>-</sup> (**b**). R<sup>+</sup>[Im]<sup>-</sup> could capture I<sub>2</sub> chemically, forming I-containing compounds together with new ILs with [I]<sup>-</sup> anion, meanwhile the new ILs could absorb I<sub>2</sub> to form polyiodide species

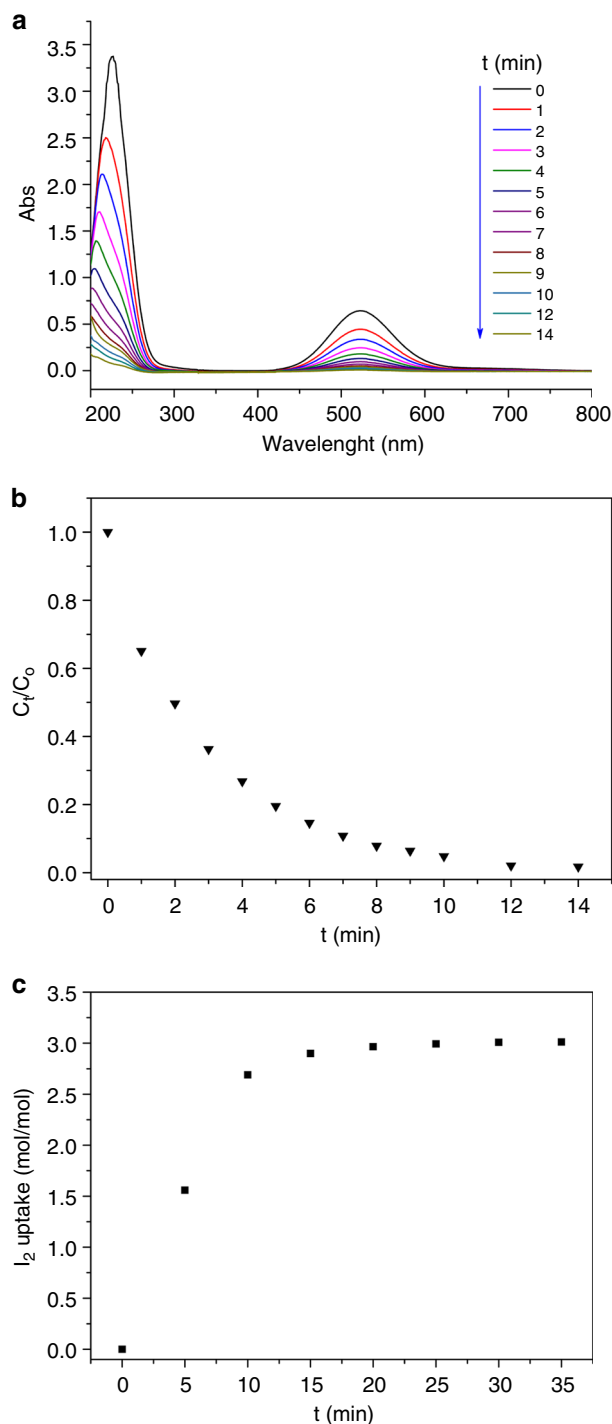


**Fig. 2** Extraction of  $I_2$  from cyclohexane solution by [Ch][Im]. **a** Time-dependent UV-visible spectra of the  $I_2$  cyclohexane solutions (50 ml, 0.01 M, 126.9 mg of  $I_2$ ) extracted by [Ch][Im] (0.3 mmol, 51 mg). **b** Time-dependent removal efficiency of  $I_2$ . **c** Time-dependent  $I_2$  uptake from cyclohexane solution (100 ml, 0.01 M) by [Ch][Im] (0.3 mmol)

viscous liquids at room temperature (Supplementary Table 1). Choline iodide ([Ch][I]) and imidazolium iodide ([ImH][I]) were synthesized via the reactions of HI with choline and imidazole in aqueous solutions, and they have the melting points of 270 °C and 204 °C, respectively.

**Extraction of  $I_2$  from cyclohexane solution by Im-ILs.** The resultant Im-ILs were first used to extract  $I_2$  from cyclohexane

solutions at 30 °C. It was found that all Im-ILs could rapidly and efficiently remove  $I_2$  from the cyclohexane solutions. As illustrated in Fig. 2, 51 mg of [Ch][Im] (0.3 mmol) almost removed  $I_2$  completely from the cyclohexane solution (0.01 M, 50 mL, 126.9 mg of  $I_2$ ) within 15 min, reaching extraction equilibrium with an  $I_2$  uptake of 3.1 mol  $I_2$  per molar IL corresponding to an  $I_2$  uptake of 4.6 g  $I_2$  per g IL (Fig. 2c). Moreover, it was found that [Ch][Im] could also rapidly and efficiently remove  $I_2$  from other solvents, for instance, n-hexane and n-heptane, affording lower  $I_2$  uptakes at extraction equilibrium of 4.2 and 2.7 g/g, respectively.

To reveal the interaction mechanism of extraction  $I_2$  by [Ch][Im], the absorbent solution obtained at the extraction equilibrium was examined by  $^1H$  and  $^{13}C$  NMR spectroscopy. Compared with those of [Ch][Im], the  $^1H$  and  $^{13}C$  NMR spectra of the absorbent solution changed significantly (Fig. 3a, b and Supplementary Fig. 3). In contrast, the signals at 141.67 and 124.22 ppm. assigned to the carbons in the [Im] $^-$  anion of [Ch][Im] disappeared and two new peaks appeared at 134.21 and 119.18 ppm., which were attributed to the carbons in [ImH] $^+$  cation according to the  $^1H$  and  $^{13}C$  NMR spectra of [ImH][I] (Supplementary Fig. 4). As shown in Fig. 3b, a new signal appeared at 89.68 ppm, which was ascribed to the carbon of C-I bond from 2,4,5-triiodoimidazole based on the  $^{13}C$  NMR spectrum of 2,4,5-triiodoimidazole (Supplementary Fig. 5). This is also confirmed by the heteronuclear singular quantum correlation (HSQC) spectrum (Supplementary Fig. 6). The heavy atom effect was responsible for the signal of I-connected carbons shifting upfield. Diffusion ordered spectroscopy (DOSY) analysis (Supplementary Fig. 7) was performed to further confirm the assignment of the carbon peaks. The diffusion sequences of the signals at 134.21 and 119.18 ppm. were similar, whereas that at 89.68 ppm. was significantly different (Supplementary Fig. 7). This indicates that the signals at 134.21 and 119.18 ppm. belonged to the same compound and the signal at 89.68 ppm. was attributed to another one, which agreed well with the above analysis. Notably, it is accepted that the carbon chemical shifts of C2 and C4/5 in 2,4,5-triiodoimidazole should be different. This is true if the NH proton is not changing position between two N atoms in 2,4,5-triiodoimidazole, whereas an exchange usually occurs in solution and on the NMR time scale, thus resulting in one peak. In addition, the signals of the carbons in [Ch] $^+$  cation only shifted slightly. The above NMR results indicate that the [Im] $^-$  anion was so active that it chemically captured  $I_2$  to form new species including [ImH] $^+$  and 2,4,5-triiodoimidazole, whereas the [Ch] $^+$  cation kept unchanged. From the  $^1H$  NMR spectra of [Ch][Im] before and after capturing  $I_2$  to reach equilibrium (Supplementary Fig. 3), it was found that the amount of H atoms in the Im ring of the absorbent solution declined to half value compared to that of [Ch][Im], implying that the [Im] $^-$  anions of [Ch][Im] were converted equally into [ImH] $^+$  cations and 2,4,5-triiodoimidazole molecules. From the above analysis, it can be deduced that during the  $I_2$  extraction process the C-H bonds in [Im] $^-$  were first iodinated to form C-I bonds accompanied with production of HI and the resultant HI subsequently induced a series of reactions to form 2,4,5-triiodoimidazole, [Ch][I], and [ImH][I]. That is,  $I_2$  was chemically captured and stored in these I-containing compounds.

To further understand the chemical reactions in the  $I_2$  extraction process, the absorbent solutions obtained at different extracting time were examined by one- and two-dimensional NMR analysis. In the spectrum of the absorbent solution obtained at 1 min, the signals at 141.67 and 124.22 ppm. assigned to C2 and C4@C5 in the [Im] $^-$  anion disappeared, accompanied with the appearance of some new signals, whereas the signals assigned to the carbons 6, 7, and 8 in [Ch] $^+$  cation shifted slightly. These results confirm that the [Im] $^-$  anion could rapidly and efficiently

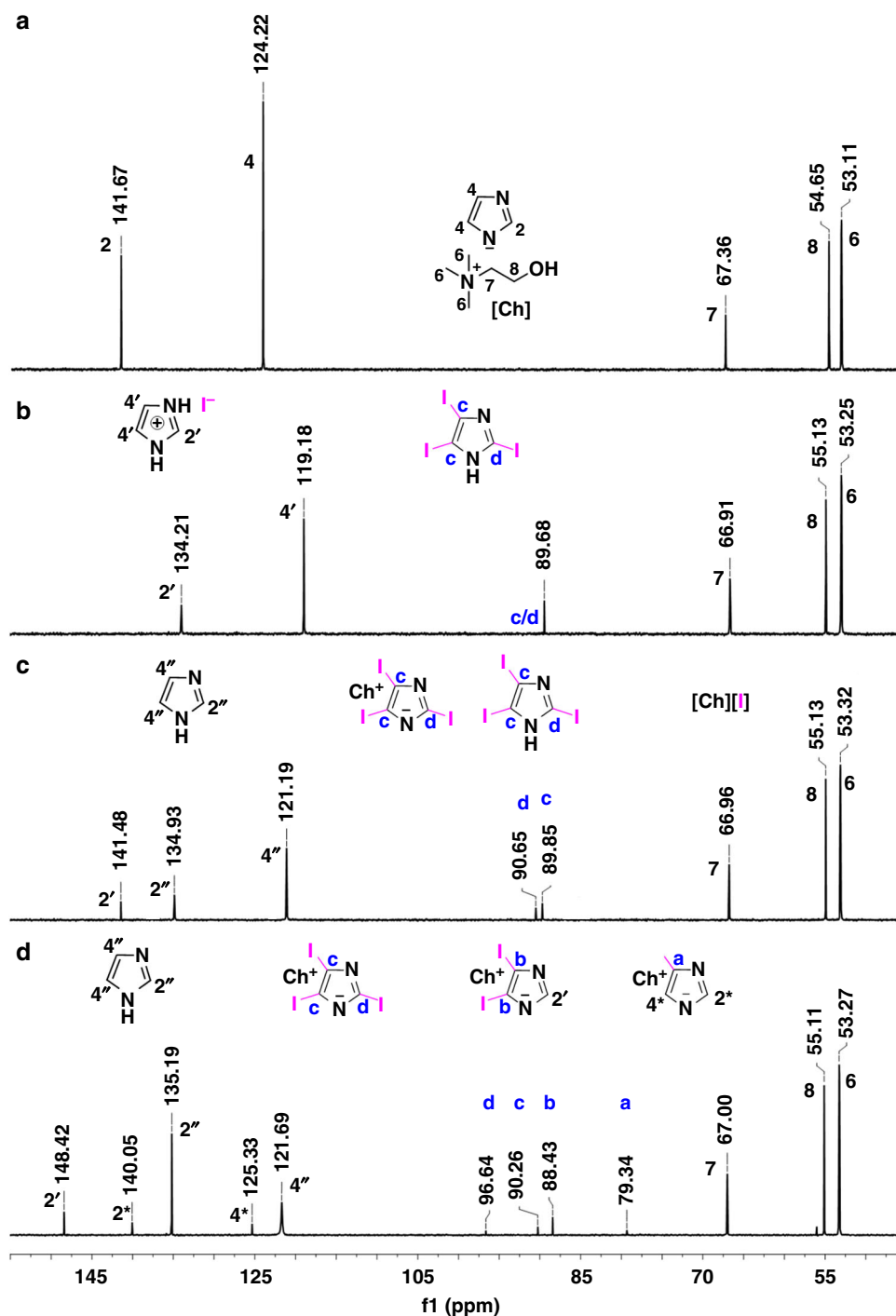


**Fig. 3**  $^{13}\text{C}$  NMR spectra of the absorbent systems. **a-d**  $^{13}\text{C}$  NMR spectra of  $[\text{Ch}][\text{Im}]$ -based absorbent systems before and after extracting  $\text{I}_2$  from cyclohexane solution at different time (**a** = 0 min, **b** = 30 min, **c** = 5 min, **d** = 1 min),  $[\text{D}_6][\text{DMSO}]$ , 0.6 mL, 298 K

capture  $\text{I}_2$  via chemical reactions, resulting in formation of new species. According to the HSQC,  $^1\text{H}$  detected heteronuclear multiple bond correlation (HMBC) and  $^{13}\text{C}$  NMR analysis (Supplementary Figs. 8, 9), the new signals at 79.34, 125.33, and 140.05 ppm. were assigned to the carbons in  $[\text{4-iodo-Im}]^-$ , whereas the signals at 121.69 and 135.19 ppm. were ascribed to the carbons in Im molecule as remarked in Fig. 3d. These findings indicate that the  $[\text{Im}]^-$  anion was iodinated to form  $[\text{4-iodo-Im}]^-$  preferentially together with HI and HI was further trapped rapidly by the unreacted  $[\text{Im}]^-$  anions to form Im molecule and  $[\text{Ch}][\text{I}]$ , as described in Fig. 4a, b. The

disappearance of signals ascribing to the  $[\text{Im}]^-$  anions also indicate that both reactions of  $[\text{Im}]^-$  with  $\text{I}_2$  to form  $[\text{4-iodo-Im}]^-$  and with HI to form Im occurred rapidly, and half of  $[\text{Im}]^-$  anions involved in the reaction with  $\text{I}_2$ , followed by the reaction of the other half with HI, identical to the results obtained from the  $^1\text{H}$  NMR spectrum of the absorbent solution at extraction equilibrium (Supplementary Figs. 3, 10). In the  $^{13}\text{C}$  NMR spectrum of this absorbent solution, the signals at 88.43 and 148.42 ppm. were ascribed to C4/C5 binding with I and C2 in  $[\text{4,5-diiodo-Im}]^-$ , respectively, whereas the signals at 96.64 and 90.26 ppm. belonged to the carbons in  $[\text{2,4,5-triiodo-Im}]^-$  anion.

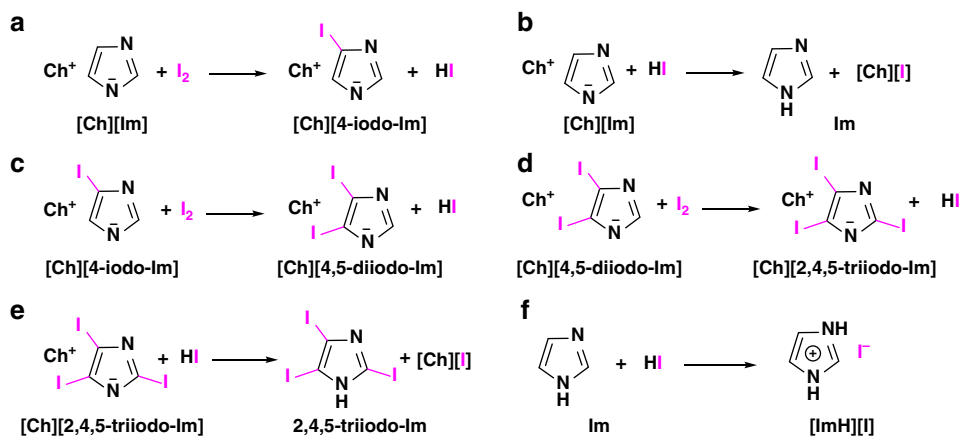


**Fig. 4** Possible reactions in the  $I_2$  extraction process by  $[Ch][Im]$ . **a** Generation of  $[Ch][4\text{-iodo-Im}]$  and HI from  $[Ch][Im]$  and  $I_2$ . **b** Reaction between  $[Ch]$  and the generated HI. **c, d** Iodination reactions of  $[Ch][4\text{-iodo-Im}]$  and  $[Ch][4,5\text{-diiodo-Im}]$ , respectively. **e** Formation of 2,4,5-triiodo-Im from  $[Ch][2,4,5\text{-triiodo-Im}]$  and HI. **f** Trap of HI by Im to form  $[ImH][I]$

**Table 1**  $I_2$  uptakes of Im-ILs at different temperatures

Entry	Absorbent	30 °C <sup>a</sup>		30 °C <sup>c</sup>		75 °C <sup>c</sup>		100 °C <sup>c</sup>	
		mol/mol	g/g	mol/mol	g/g	mol/mol	g/g	mol/mol	g/g
1	$[Ch][Im]$	3.1 <sup>b</sup>	4.6	5.9	8.7	8.8	13.0	11.8	17.5
2	$[N_{4444}][Im]$	-	-	-	-	8.1	6.6	14.2	11.6
3	$[Ch][2\text{-MIm}]$	3.1 <sup>b</sup>	4.2	2.8	3.8	9.0	12.3	11.5	15.8
4	$[Ch][4\text{-MIm}]$	3.0 <sup>b</sup>	4.1	3.9	5.3	8.2	11.2	10.3	14.1
5	$[Ch][2,4\text{-DMIm}]$	3.1 <sup>b</sup>	3.9	5.2	6.6	7.7	9.8	8.2	10.4
6	$[Ch][I]$	-	-	-	-	5.2	5.7	6.5	7.1
7	$[ImH][I]$	-	-	-	-	5.8	7.5	7.5	9.7

<sup>a</sup>Extracting  $I_2$  from cyclohexane solution (100 ml, 0.01 M) by Im-ILs (0.3 mmol) at room temperature

<sup>b</sup>Determined by UV/Vis spectroscopy

<sup>c</sup> $I_2$  vapor absorption capacity by the Im-ILs at different temperatures: absorbent, 0.3 mmol; absorbing time, 12 h

These results suggest that the C–H bonds in  $[4\text{-iodo-Im}]^-$  and  $[4,5\text{-diiodo-Im}]^-$  anions further reacted with  $I_2$  quickly to form  $[2,4,5\text{-triiodo-Im}]^-$ , as shown in Fig. 4c, d. In the spectrum of the absorbent solution obtained at 5 min, the signals to the carbons of  $[4\text{-iodo-Im}]^-$  and  $[4,5\text{-diiodo-Im}]^-$  disappeared, whereas the signals to C2 and C4/5 in the iodinated imidazolium ring enhanced and became closer. This further indicates that not only the reactions shown in Fig. 4c, d took place but also that in Fig. 4e occurred, based on the  $^{13}C$  NMR spectra of the mixture of 2,4,5-triiodoimidazole and  $[Ch][2,4,5\text{-triiodo-Im}]$  with different molar ratio (Supplementary Fig. 11). In the  $^{13}C$  NMR spectrum of the absorbent solution at extraction equilibrium (Fig. 3b), the peaks at 134.21 and 119.18 ppm. were ascribed to the carbons in  $[ImH]^+$ , suggesting the formation of  $[ImH][I]$  from the reaction of Im with HI (Fig. 4f).

To further verify the reactions illustrated in Fig. 4, the control reaction of HI (2 mmol) with  $[Ch][Im]$  (1 mmol) was conducted in aqueous solution at room temperature. Indeed, the reaction occurred rapidly and  $[Ch][I]$  was obtained together with  $[ImH][I]$ , as confirmed by the NMR analysis (Supplementary Figs. 4 and 12). These results indicate that during the  $I_2$  extraction process from cyclohexane solution, the generated HI could be trapped by  $[Ch][Im]$  to form  $[Ch][I]$  and  $[ImH][I]$ . Notably, 2,4,5-triiodoimidazole could be isolated from the absorbent solution, verified by the NMR analysis (Supplementary Figs. 5, 13), which confirmed the reaction shown in Fig. 4e.

Based on the mass balance and the equations shown in Fig. 4, the molar ratio of  $[Ch][I]:[Im][I]:2,4,5\text{-triiodoimidazole}$  should be 1:0.5:0.5 at the reaction equilibrium, which means that 1.5 mol

of  $I_2$  can be theoretically captured by per molar  $[Ch][Im]$ . In fact, the  $I_2$  uptake by  $[Ch][Im]$  reached 3.1 mol/mol (Table 1). This suggests that the mixture of  $[Ch][I] + [Im][I] + 2,4,5\text{-triiodoimidazole}$  contributed to the extraction of  $I_2$  from the cyclohexane solution as well.

Encouraged by the above results, other Im-ILs shown in Fig. 1a were also used to extract  $I_2$  from cyclohexane solutions at 30 °C and the results are included in Table 1. Obviously, these Im-ILs could efficiently extract  $I_2$  with high efficiency and the  $I_2$  uptake of each Im-IL was almost the same. These results imply that the anions of these Im-ILs might behave similarly in extracting  $I_2$ . NMR analyses (Supplementary Fig. 14) indicate that besides all the  $Csp^2\text{-H}$  bonds in the Im ring, one  $Csp^3\text{-H}$  bond in each  $-\text{CH}_3$  of  $[2\text{-MIm}]^-$ ,  $[4\text{-MIm}]^-$ , and  $[2,4\text{-DMIm}]^-$  anions was iodinated to form  $-\text{CH}_2\text{I}$ , suggesting that the  $-\text{CH}_3$  group in these anions was active to attract  $I_2$ . That is, similar to  $[Im]^-$ , each anion,  $[2\text{-MIm}]^-$ ,  $[4\text{-MIm}]^-$ , and  $[2,4\text{-DMIm}]^-$ , has three C–H bonds that can react with  $I_2$ , resulting in the chemical capture of  $I_2$ . Similarly, the generated HI was also found to induce a series of reactions to form corresponding I-substituted imidazoles and ILs with  $[I]^-$  anions, which were illustrated in Supplementary Fig. 15.

**DFT calculation.** To understand the reactivity of the anions of these Im-ILs, we calculated the Hirshfeld charges of carbons in the Im ring of imidazole,  $[Im]^-$  and  $[ImH]^+$ , and the results are shown in Supplementary Fig. 16. In general, the carbon site possessing more negative Hirshfeld charge has stronger ability to attract electrophiles and is thus more possible to be the reactive

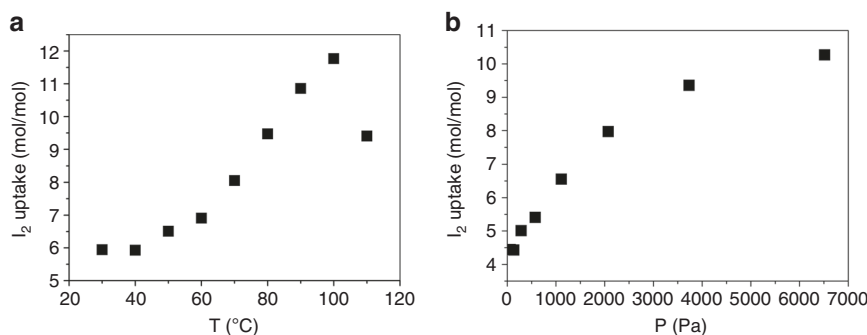


**Fig. 5** Influences of temperature and vapor pressure on I<sub>2</sub> uptakes. Dependence of I<sub>2</sub> uptakes of [Ch][Im] on temperature (**a**) and on the vapor pressures of I<sub>2</sub> (**b**)

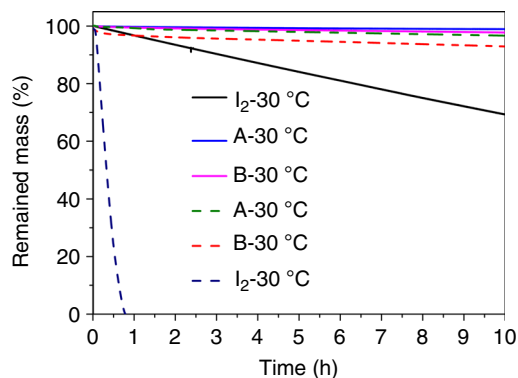


**Fig. 6** TGA curves of [Ch][Im] after absorbing I<sub>2</sub>. Sample **A** presents the IL absorbing 3.1 mol/mol of I<sub>2</sub> from cyclohexane solution and sample **B** presents the IL absorbing 5.9 mol/mol of I<sub>2</sub> vapor; N<sub>2</sub> sweeping rates: 40 mL/min at 30 °C, 5 mL/min at 100 °C

site<sup>33,34</sup>. The calculation results indicate that the Hirshfeld charges of the carbon atoms in [Im]<sup>-</sup> become more negative compared with those in imidazole, whereas those in [ImH]<sup>+</sup> are more positive. Similarly, the Hirshfeld charges of the carbons, especially the methyl carbons, in the [methyl-substituted-Im]<sup>-</sup> anion are also negative (Supplementary Fig. 16). These results imply that both Csp<sup>2</sup>-H and Csp<sup>3</sup>-H in the anions have the capability to react with I<sub>2</sub>. Therefore, it can be deduced that Im anion-directed electron redistribution is favorable to promoting C-H bond activation, thus providing multiple-sites to capture I<sub>2</sub> chemically with different reactivity.

**I<sub>2</sub> vapor capture by [Im]-ILs.** As I<sub>2</sub> capture is generally performed in gas atmosphere, the resultant Im-ILs were applied in capturing I<sub>2</sub> vapor and the results are shown in Table 1. Obviously, each Im-IL could capture I<sub>2</sub> with a very high capacity, much higher than those of various absorbents or adsorbents reported in literature (Supplementary Table 2)<sup>6,9,14,15</sup>. For example, using [Ch][Im] as the absorbent, its I<sub>2</sub> capture capacity increased with temperature in the range of 30–100 °C, reaching the highest value of 11.8 mol/mol (i.e., 17.5 g/g) at 100 °C. Further increasing temperature caused decline in I<sub>2</sub> capture capacity, decreasing to 9.4 mol/mol at 110 °C (Fig. 5a).

As described above, the I<sub>2</sub> capture capacity of [Ch][Im] includes two parts: the chemical capture capacity of 1.5 mol I<sub>2</sub> per molar IL and the I<sub>2</sub> uptake by the mixture of [Ch][I] + [ImH][I] + 2,4,5-triiodoimidazole. The latter is actually the I<sub>2</sub> solubility in the mixture. In general, the solubility of a solute in a solvent is related to its vapor pressure. Calculating the vapor pressures of I<sub>2</sub>

at different temperatures in the range of 30–100 °C (Supplementary Table 3 and Supplementary Fig. 17), the dependence of the I<sub>2</sub> uptakes of [Ch][Im] on its vapor pressures is plotted in Fig. 5b. Obviously, the I<sub>2</sub> uptakes of [Ch][Im] increased with the I<sub>2</sub> vapor pressures, suggesting that higher vapor pressure, i.e., higher temperature, is favorable to the I<sub>2</sub> absorption by the mixture of [Ch][I], [ImH][I], and 2,4,5-triiodoimidazole. However, further increasing temperature to 110 °C, the I<sub>2</sub> uptake of [Ch][Im] reduced, which may be ascribed to the weaker interactions among I<sub>2</sub> and the absorbent molecules at higher temperature.

**I<sub>2</sub> storage reliability.** Besides rapid and efficient I<sub>2</sub> absorption, it is also very important for volatile I<sub>2</sub> to be stably stored in the absorbent system for a long time. To examine the I<sub>2</sub> storage reliability in the [Ch][Im]-based absorbent system, TGA analysis with N<sub>2</sub> sweeping was performed on sample **A** and sample **B** as shown in Fig. 6. Clearly, the mass losses of these samples were hardly observed at 30 °C under a N<sub>2</sub> sweeping flow rate of 40 mL/min for 10 h, whereas pure I<sub>2</sub> powder showed ~30 wt% mass loss under the same condition. At 100 °C, only < 5% of mass losses for sample **A** and sample **B** were observed after N<sub>2</sub> sweeping with a flow rate of 5 mL/min for 10 h, whereas the same amount of powdered I<sub>2</sub> almost completely evaporated within 50 min. These results indicate that even at high temperature (e.g., 100 °C), the absorbent system still has relatively reliable capability to store I<sub>2</sub>. Compared with the reported I<sub>2</sub> absorbents in literature<sup>14,15</sup>, this IL absorbent system exhibits much better performance for I<sub>2</sub> storage.

**Melting points of [Ch][Im]-based absorbent systems.** [Ch][I], [ImH][I], and 2,4,5-triiodoimidazole are solids at room temperature with melting points at 263, 204, and 189 °C, respectively. In the process of I<sub>2</sub> absorption by [Ch][Im], the mixture of [Ch][I], [ImH][I], and 2,4,5-triiodoimidazole was formed, but they displayed liquid state after capturing I<sub>2</sub> at room temperature. This indicates that the absorbed I<sub>2</sub> considerably decreased the melting point of the [Ch][I] + [ImH][I] + 2,4,5-triiodoimidazole mixture. To explore the influence of I<sub>2</sub> on the melting points of [Ch][I] and [ImH][I], we determined the phase diagrams of [ImH][I]-I<sub>2</sub> and [Ch][I]-I<sub>2</sub> binaries. It was found that [Ch][I] and [ImH][I] could form low-temperature eutectic salts with I<sub>2</sub>, significantly decreasing the melting points of [Ch][I]-I<sub>2</sub> and [ImH][I]-I<sub>2</sub> binaries (Supplementary Figs. 18, 19). Moreover, the mixture of [Ch][I], [ImH][I], and 2,4,5-triiodoimidazole with a molar ratio of 1:0.5:0.5 was found to have a melting point of 78 °C, much lower than that of each compound, and the melting point further decreased after capturing I<sub>2</sub>. Therefore, the above findings suggest that although [Ch][I] and [ImH][I] are solids with high melting points, they are highly efficient absorbents for I<sub>2</sub>, because they can form low-temperature eutectic salts with I<sub>2</sub>.

**Analysis on iodide species.** In contrast, in the case of extracting  $I_2$  from cyclohexane solution the  $I_2$  capture capacity of [Ch][Im] reached 3.1 mol/mol at the extraction equilibrium at 30 °C and it could not increase further even if enough amount of  $I_2$  was present in the cyclohexane solution, whereas it reached 5.9 mol/mol in the case of capturing  $I_2$  vapor. These results suggest that iodide species may exist in different forms in the IL solutions in these two cases. To reveal the forms of the iodide species in the IL solutions, we conducted the electrospray ionization mass spectrometry (ESI-MS) in negative mode on the IL solutions (Supplementary Figs. 20, 21). It was observed that the iodide species mainly existed as 2,4,5-triiodoimidazole,  $I^-$  and  $I_3^-$  in the extraction solution, whereas besides these species polyiodide species (including  $I_5^-$ ,  $I_7^-$ ) combined with IL cations were present in the IL solution absorbing  $I_2$  vapor, identical to that reported in literature<sup>35</sup>. The ESI-MS results enclosed why the absorption capacity of the IL capturing  $I_2$  vapor was much higher than that extracting  $I_2$  from cyclohexane solution.

## Discussion

A series of Im-ILs were designed, which were found to be capable of rapidly and efficiently capturing  $I_2$  via the reactions of the Im anions with  $I_2$  and the formation of polyiodide species (Fig. 1b), showing high  $I_2$  capture capacity. Moreover, the Im-ILs systems were safe materials for the storage of  $I_2$ , and they could be tolerant to high temperature (e.g., 100 °C). This work presents green absorbent systems to capture  $I_2$  rapidly and efficiently, which have promising potential applications in capturing radioactive  $I_2$  from the nuclear waste with stable storage.

## Methods

**Materials.** Iodine, choline chloride, imidazole, 2-methylimidazole, 4-methylimidazole, 2,4-dimethylimidazole, tetrabutylammonium bromide, and ion exchange resin (Ambersep1r 900(OH)) were obtained from Beijing Innochem Science & Technology Co., Ltd. and J&K Scientific Ltd., respectively. All chemicals were used without further purification.

**General procedure for the synthesis of Im-ILs.** The ILs as depicted in Fig. 1a, including [Ch][Im], [Ch][2-MIm], [Ch][4-MIm], and [Ch][2,4-DMIm] were prepared by neutralizing [Ch][OH] with corresponding weak proton donors. Typically, for the synthesis of [Ch][Im], an ethanol solution of [Ch][OH] was first obtained from [Ch][Cl] via anion-exchange resin. To the ethanol solution of [Ch][OH] equimolar imidazole was added and the mixture was then stirred at room temperature for 24 h. Subsequently, ethanol and generated water were distilled off at 70 °C under reduced pressure. The obtained [Ch][Im] was dried in vacuum for 24 h at 70 °C to remove trace amount of water. The water content of these ILs was determined with a Karl Fisher titration and found to be < 0.1 wt%.

**Typical procedure for  $I_2$  extraction from cyclohexane solution.** In a typical experiment, [Ch][Im] (51 mg, 0.3 mmol) was added into a cyclohexane solution containing  $I_2$  (0.01 M, 100 ml) in 250 mL flask equipped with a magnetic stirrer at r.p.m. of 400 r/min. The  $I_2$  quantitative analysis at different extraction time was conducted by UV/Vis spectroscopy analysis. The intensity of absorption peaks at  $\lambda = 523$  nm is proportional to the quantity of  $I_2$ .

**$I_2$  vapor capture.** Typically, [Ch][Im] (26 mg, 0.15 mmol) loaded in a pre-weighed culture dish (5 cm in diameter) was exposed to an  $I_2$  vapor environment in a desiccator at a given temperature, in which  $I_2$  crystals (2 g) were placed in lieu of the desiccant. The amount of  $I_2$  absorbed was determined by an analytical balance within an accuracy of  $\pm 0.0001$  g.

**Characterization.**  $^1H$  and  $^{13}C$  NMR analyses were performed on a Bruker Avance NMR spectrometer (400 MHz) (Germany) with  $[D_6][DMSO]$  as a solvent. The DOSY, HSQC, and HMBC spectra were collected on a Bruker Avance NMR (600 MHz) (Germany) with  $[D_6][DMSO]$  as a solvent. The thermogravimetric analysis was conducted at a Perkinelmer TGA 4000. The UV-vis analysis was performed at TU-1901 spectrophotometer.

**DFT calculation.** Stable structures of Im in different environment were optimized at the B3LYP/6-311 + g(d,p) level using Gaussian 09 package. Solvation

(cyclohexane) corrections were calculated by a self-consistent reaction field using the CPCM model. Hirshfeld atomic charge was calculated based on the wave function of the optimum structures using the Multiwfn code.

**The calculation of the vapor pressures of  $I_2$  at different temperatures.** The temperature for the indicated pressure of  $I_2$  solid (Supplementary Table 3) was obtained from the CRC handbook of chemistry and physics (90th edition). The temperature–vapor pressures (Supplementary Fig. 17) curve fits with the Clausius–Clapeyron equation ( $\ln P = -\frac{\Delta H}{RT} + C$ ), which was then used for calculating the vapor pressures of  $I_2$  at different temperatures in the range of 30–100 °C.

## Data availability

The data supporting the findings of this study are available within the article and its Supplementary Information files. All other relevant source data are available from the corresponding author upon reasonable request.

Received: 5 June 2018 Accepted: 25 September 2018

Published online: 22 October 2018

## References

- Gralla, F., Abson, D. J., Möller, A. P., Lang, D. J. & von Wehrden, H. Energy transitions and national development indicators: a global review of nuclear energy production. *Renew. Sustain. Energy Rev.* **70**, 1251–1265 (2017).
- Brimmo, A. T., Sodiq, A., Sofela, S. & Kolo, I. Sustainable energy development in Nigeria: wind, hydropower, geothermal and nuclear. *Renew. Sustain. Energy Rev.* **74**, 474–490 (2017).
- Parshamoni, S., Sanda, S., Jena, H. S. & Konar, S. Tuning  $CO_2$  uptake and reversible iodine adsorption in two isoreticular MOFs through ligand functionalization. *Chem. Asian J.* **10**, 653–660 (2015).
- Yao, R. X., Cui, X., Jia, X. X., Zhang, F. Q. & Zhang, X. M. A luminescent zinc (II) metal–organic framework (MOF) with conjugated  $\pi$ -electron ligand for high iodine capture and nitro-explosive detection. *Inorg. Chem.* **55**, 9270–9275 (2016).
- Li, B. et al. Capture of organic iodides from nuclear waste by metal-organic framework-based molecular traps. *Nat. Commun.* **8**, 485 (2017).
- Geng, T. M., Zhu, Z. M., Zhang, W. Y. & Wang, Y. A nitrogen-rich fluorescent conjugated microporous polymer with triazine and triphenylamine units for high iodine capture and nitro aromatic compound detection. *J. Mater. Chem. A* **5**, 7612–7617 (2017).
- Qian, X. et al. Capture and reversible storage of volatile iodine by novel conjugated microporous polymers containing thiophene units. *ACS Appl. Mater. Inter.* **8**, 21063–21069 (2016).
- Liao, Y. Z., Weber, J., Mills, B. M., Ren, Z. & Faul, C. F. J. Highly efficient and reversible iodine capture in hexaphenylbenzene-based conjugated microporous polymers. *Macromolecules* **49**, 6322–6333 (2016).
- Yan, Z. J., Yuan, Y., Tian, Y. Y., Zhang, D. M. & Zhu, G. S. Highly efficient enrichment of volatile iodine by charged porous aromatic frameworks with three sorption sites. *Angew. Chem. Int. Ed.* **54**, 12733–12737 (2015).
- Lin, Y. X. et al. An elastic hydrogen-bonded cross-linked organic framework for effective iodine capture in water. *J. Am. Chem. Soc.* **139**, 7172–7175 (2017).
- Jie, K. C. et al. Reversible iodine capture by nonporous pillar[6]arene crystals. *J. Am. Chem. Soc.* **139**, 15320–15323 (2017).
- Sun, H. X. et al. Innovative nanoporous carbons with ultrahigh uptakes for capture and reversible storage of  $CO_2$  and volatile iodine. *J. Hazard. Mater.* **321**, 210–217 (2017).
- Scott, S. M., Hu, T., Yao, T. K., Xin, G. Q. & Lian, J. Graphene-based sorbents for iodine-129 capture and sequestration. *Carbon N. Y.* **90**, 1–8 (2015).
- Li, G. F. et al. Highly efficient  $I_2$  capture by simple and low-cost deep eutectic solvents. *Green. Chem.* **18**, 2522–2527 (2016).
- Yan, C. Y. & Mu, T. C. Investigation of ionic liquids for efficient removal and reliable storage of radioactive iodine: a halogen-bonding case. *Phys. Chem. Chem. Phys.* **16**, 5071–5075 (2014).
- Chen, Y., Zhang, F. G. & Xue, Z. M. Iodine capture by ionic liquids and recovery by compressed  $CO_2$ . *J. Mol. Liq.* **223**, 202–208 (2016).
- Cao, B. B. et al. Experiment and DFT studies on radioiodine removal and storage mechanism by imidazolium-based ionic liquid. *J. Mol. Graph. Modell.* **64**, 51–59 (2016).
- Lu, Y. et al. Coherent-interface-assembled  $Ag_2O$ -anchored nanofibrillated cellulose porous aerogels for radioactive iodine capture. *ACS Appl. Mater. Inter.* **8**, 29179–29185 (2016).
- Chapman, K. W., Chupas, P. J. & Nenoff, T. M. Radioactive iodine capture in silver-containing mordenites through nanoscale silver iodide formation. *J. Am. Chem. Soc.* **132**, 8897–8899 (2010).

20. Solis-Ibarra, D. & Karunadasa, H. I. Reversible and irreversible chemisorption in nonporous-crystalline hybrids. *Angew. Chem. Int. Ed.* **53**, 1039–1042 (2014).
21. Funabiki, A. et al. Reversible iodine absorption by alkali-TCNQ salts with associated changes in physical properties. *J. Mater. Chem.* **22**, 8361–8366 (2012).
22. Mohanambe, L. & Vasudevan, S. Insertion of iodine in a functionalized inorganic layered solid. *Inorg. Chem.* **43**, 6421–6425 (2004).
23. Zhang, Z. R., Song, J. L. & Han, B. X. Catalytic transformation of lignocellulose into chemicals and fuel products in ionic liquids. *Chem. Rev.* **117**, 6834–6880 (2017).
24. Egorova, K. S., Gordeev, E. G. & Ananikov, V. P. Biological activity of ionic liquids and their application in pharmaceuticals and medicine. *Chem. Rev.* **117**, 7132–7189 (2017).
25. Cui, G. K., Wang, J. J. & Zhang, S. J. Active chemisorption sites in functionalized ionic liquids for carbon capture. *Chem. Soc. Rev.* **45**, 4307–4339 (2016).
26. Seitkalieva, M. M., Kashin, A. S., Egorova, K. S. & Ananikov, V. P. Ionic liquids as tunable toxicity storage media for sustainable chemical waste management. *ACS Sustain. Chem. Eng.* **6**, 719–726 (2018).
27. Wang, C. M. et al. Tuning the basicity of ionic liquids for equimolar CO<sub>2</sub> capture. *Angew. Chem. Int. Ed.* **50**, 4918–4922 (2011).
28. Luo, X. Y. et al. Significant improvements in CO<sub>2</sub> capture by pyridine-containing anion-functionalized ionic liquids through multiple-site cooperative interactions. *Angew. Chem. Int. Ed.* **53**, 7053–7057 (2014).
29. Chen, F. F. et al. Multi-molar absorption of CO<sub>2</sub> by the activation of carboxylate groups in amino acid ionic liquids. *Angew. Chem. Int. Ed.* **55**, 7166–7170 (2016).
30. Chen, K. H., Shi, G. L., Zhou, X. Y., Li, H. R. & Wang, C. M. Highly efficient nitric oxide capture by azole-based ionic liquids through multiple-site absorption. *Angew. Chem. Int. Ed.* **55**, 14364–14368 (2016).
31. Tao, D. J. et al. Highly efficient carbon monoxide capture by carbanion-functionalized ionic liquids through C-site interactions. *Angew. Chem. Int. Ed.* **56**, 6843–6847 (2017).
32. Cui, G. K. et al. Tuning anion-functionalized ionic liquids for improved SO<sub>2</sub> capture. *Angew. Chem. Int. Ed.* **52**, 10620–10624 (2013).
33. Liu, S. B. Quantifying reactivity for electrophilic aromatic substitution reactions with Hirshfeld charge. *J. Phys. Chem. A* **119**, 3107–3111 (2015).
34. Liu, S. B., Rong, C. Y. & Lu, T. Information conservation principle determines electrophilicity, nucleophilicity, and regioselectivity. *J. Phys. Chem. A* **118**, 3698–3704 (2014).
35. Fei, Z. F., Bobbink, F. D., Păunescu, E., Scopelliti, R. & Dyson, P. J. Influence of elemental iodine on imidazolium-based ionic liquids: solution and solid-state effects. *Inorg. Chem.* **54**, 10504–10512 (2015).

## Acknowledgements

This work was financially supported by the National Key Research and Development Program of China (Grant Number 2017YFA0403101) and the National Natural Science Foundation of China (Grant Numbers 21733011 and 21533011).

## Author contributions

Z.M.L. and J.J.W. proposed the project. R.P.L., Y.C., and Z.Y.L. synthesized the ILs and conducted the absorption experiments and mechanism study. Y.F.Z. designed the study and performed the DFT calculation. B.X.H. was involved in scientific discussion. All authors contributed to the writing of the manuscript.

## Additional information

**Supplementary information** accompanies this paper at <https://doi.org/10.1038/s42004-018-0067-2>.

**Competing interests:** The authors declare no competing interests.

**Reprints and permission** information is available online at <http://npg.nature.com/reprintsandpermissions/>

**Publisher's note:** Springer Nature remains neutral with regard to jurisdictional claims in published maps and institutional affiliations.



**Open Access** This article is licensed under a Creative Commons

Attribution 4.0 International License, which permits use, sharing, adaptation, distribution and reproduction in any medium or format, as long as you give appropriate credit to the original author(s) and the source, provide a link to the Creative Commons license, and indicate if changes were made. The images or other third party material in this article are included in the article's Creative Commons license, unless indicated otherwise in a credit line to the material. If material is not included in the article's Creative Commons license and your intended use is not permitted by statutory regulation or exceeds the permitted use, you will need to obtain permission directly from the copyright holder. To view a copy of this license, visit <http://creativecommons.org/licenses/by/4.0/>.

© The Author(s) 2018